

## Supporting Information

# Efficacious and sustained release of an anticancer drug mitoxantrone from new covalent organic frameworks using protein corona

Subhajit Bhunia,<sup>b,†</sup> Pranay Saha,<sup>c,†</sup> Parikshit Moitra,<sup>d</sup> Matthew A. Addicoat,<sup>e</sup> and Santanu Bhattacharya<sup>\*ac</sup>

<sup>a</sup>Department of Organic Chemistry, Indian Institute of Science, Bangalore, 560012, India, E-mail: sb@iisc.ac.in, sb23in@yahoo.com

<sup>b</sup>Department of Chemistry & Biochemistry, University of Texas at El Paso, El Paso, Texas 79968, United States

<sup>c</sup>School of Applied and Interdisciplinary Sciences, Indian Association for the Cultivation of Science, Kolkata, West Bengal 700032, India

<sup>d</sup>Department of Pediatrics, Center for Blood Oxygen Transport and Hemostasis, University of Maryland Baltimore School of Medicine, Health Sciences Facility III, Baltimore, Maryland 21201, United States

<sup>e</sup>School of Science and Technology, Nottingham Trent University, Nottingham, NG11 8NS, UK.

<sup>†</sup>These authors contributed equally to this work.

**KEYWORDS** Covalent organic framework, perylene based 2D materials, protein corona, anticancer drug delivery

## Table of Contents

<b>Section S1</b>	<i>Characterization, methods and techniques</i>	<b>S3-S7</b>
<b>Section S2</b>	<i>Synthetic Procedures of building blocks and <sup>1</sup>H NMR</i>	<b>S7-S10</b>
<b>Section S3</b>	<i>Computational Details</i>	<b>S10-S24</b>
<b>Section S4</b>	<i>Fourier transform infrared spectroscopy (FT-IR)</i>	<b>S26</b>
<b>Section S5</b>	<i><sup>13</sup>C solid state CP/MAS NMR</i>	<b>S26</b>
<b>Section S6</b>	<i>Thermogravimetric analysis (TGA)</i>	<b>S27</b>
<b>Section S7</b>	<i>Ultrahigh resolution transmission electron microscopy (UHR-TEM) analysis</i>	<b>S28</b>
<b>Section S8</b>	<i>FT-IR spectra of Mitoxantrone (MXT) and MXT loaded COF</i>	<b>S29</b>
<b>Section S9</b>	<i>Change of absorption of MXT upon binding with PER@PDA-COF-1</i>	<b>S29</b>
<b>Section S10</b>	<i>Change of fluorescent spectra of PER@PDA-COF-1 upon binding with MXT and the linear regression plot</i>	<b>S30</b>
<b>Section S11</b>	<i>Binding constant calculation (<math>K_{sv}</math>) for the MXT binding with COF</i>	<b>S30</b>
<b>Section S12</b>	<i>Job's plot analysis of binding of proteins</i>	<b>S31</b>
<b>Section S13</b>	<i>Comparative study of the "Turn-ON" response of PER@PDA-COF-1 towards various proteins</i>	<b>S31</b>
<b>Section S14</b>	<i>Cyclic voltammetry</i>	<b>S32</b>
<b>Section S15</b>	<i>Effect of urea and temperature on the stability of System-II</i>	<b>S32</b>
<b>Section S16</b>	<i>Effect of pH on the stability of albumin/COF nano assembly</i>	<b>S33</b>
<b>Section S17</b>	<i>Effect of temperature and urea on MXT release by system I, system II and system III.</i>	<b>S33</b>
<b>Section S18</b>	<i>Comparison of Proteinase-K stability of System-II and System-III</i>	<b>S34</b>
<b>Section S19</b>	<i>Comparative time dependent cellular release profile of MXT from system-I, system-II, system-III and MXT only</i>	<b>S34</b>
<b>Section S20</b>	<i>Extracellular and intracellular distribution of Time dependent released MXT by MXT-PER@PDA-COF and HSA-PER@PDA-COF-1.</i>	<b>S35</b>
<b>Section S21</b>	<i>Fluorescent microscopy study of cellular internalization of MXT.</i>	<b>S35</b>
<b>Section S22</b>	<i>Visualization of extracellular and intracellular MXT (CT-26 cell line)</i>	<b>S36</b>
<b>Table S1</b>	<i>Comparative percentage of hemolysis and clotting time using different biosystem along with system I, system II and system III.</i>	<b>S36</b>
<b>Section S23</b>	<i>Mice tumor Models and In vivo Studies</i>	<b>S37-S38</b>
<b>Section S24</b>	<i>Blood biochemistry</i>	<b>S38-S39</b>
<b>Section S25</b>	<i>Preparation of tissue lysate and bio-distribution studies</i>	<b>S38-39</b>
<b>Section S26</b>	<i>Clearance Pathway</i>	<b>S40</b>
<b>References</b>		<b>S40</b>

## **Section S1: Methods**

### **1.1. Characterization of Materials**

<sup>1</sup>H and <sup>13</sup>C NMR spectra were recorded using Bruker DPX-300 NMR spectrometer. The chemical shift ( $\delta$  in ppm) was recorded with respect to the residual proton of the solvent as standard. Multiplicities are written as s (singlet), d (doublet), t (triplet), m (multiplet) and br (broad). X-Ray diffraction patterns of the powder samples were obtained with a Panalytical X'Part<sup>3</sup> powder diffractometer using Cu-K $\alpha$  (0.15406 nm) radiation. The solid state cross-polarization magic angle spinning (CP-MAS) <sup>13</sup>C NMR spectrum was recorded using a 100 MHz Bruker Avance II spectrometer at mass frequency of 8 kHz. FT-IR spectra were recorded using a Nicolet MAGNA-FT IR 750 Spectrometer Series II. Porosity measurement using volumetric N<sub>2</sub> adsorption/desorption was carried out by using Autosorb 1 (quantachrome, USA) instrument. The activation of the sample , the sample cell was outgassed at 130°C for 12 h under vacuum to remove all the entrapped solvent impurities. NLDFT pore size distribution was obtained by applying slit/cylindrical pore model on the N<sub>2</sub> adsorption/desorption isotherm. Thermo gravimetric (TGA) and differential thermal analyses (DTA) of the samples have been done by TGA Instruments thermal analyzer (TA-SDT Q-600). Elemental mapping and morphological analysis have been done using Hitachi S-5200 field-emission scanning electron microscope. The ultra-high resolution transmission electron microscopy (UHR-TEM) of the sample was done using a JEOL JEM 2010 transmission electron microscope operating at 200 kV. For the electron microscopy analysis the sample was dispersed in absolute ethanol and then drop coated on the carbon coated copper grid.

### **1.2. UV-Visible Spectroscopy**

Loading of mitoxantrone into PER@PDA-COF-1 was measured by UV-visible absorption spectroscopy. Optical absorption spectra were recorded using Shimadzu UV-2600 UV-Vis spectrophotometer. For measuring the generation of reactive oxygen species (ROS) inside the cells, UV-vis spectra were measured in 96 well plates in Biotek epoch 2 microplate reader instrument.

### **1. 3. Fluorescence Spectroscopy**

Fluorescence spectra of various samples were recorded in Horiba Fluoromax-4 spectrofluorometer. Mitoxantrone concentrations released inside the cells in different culture conditions were measured. For larger number of samples Horiba Fluoromax-4 was used along with MicroMax 384 plate reader.

### **1. 4. Fluorescent lifetime analysis of PER@PDA-COF-1 with HSA**

Fluorescence lifetime spectra were recorded in Horiba Jobin Yvon IBH with JY-IBH 5000M monochromator. Time-resolved fluorescence measurements were achieved with an excitation wavelength of 440 nm using a source of NaboLED-440L (pd<200ps). Instrumental response function (IRF) of the time correlated single-photon counting (TCSPC) of HSA-MXT-PER@PDA-CON-1 complex was 45 ps. Emission wavelength was set at 473 nm for MXT-PER@PDA-CON-1. The pico-timing amplifier and discriminator employed was Ortec 9327. The sample solutions were taken in cuvette separately and the detection was done using a MCP PMT Hamamatsu R3809 multichannel plate multiplier. For data acquisition and overall controlling DataStation v2.3 and for fluorescence decay analyses DAS6 softwares were used. Time calibrations were calculated using bi-exponentials against the IRF with FWHM  $\sim 2.7475E^{-2}$  ns/ch.

### **1. 5. Atomic Force Microscopy**

AFM images were taken in Veeco diCP II AP0100 atomic force microscope with 0.01-0.025 ohm-cm-antimony-doped-silicon cantilever having a thickness  $\times$  length  $\times$  width of 3.75  $\mu\text{m} \times$  125  $\mu\text{m} \times$  35  $\mu\text{m}$  and having a frequency of 300 KHz and Young's modulus of 40 N/m<sup>2</sup>. PER@PDA-COF-1 (0.25 mg/ml) in PBS was drop coated over 0.8 cm<sup>2</sup> freshly cleaved mica sheets.

#### *1.5.1. Bare PER@PDA-COF-1 nanosheet preparation*

2 mg of PER@PDA-COF-1 was dispersed in 1 mL mili-Q water via bath sonication during 30 min. Then the solution was centrifuged at 4000 rpm and collected the supernatant solution. Then the supernatant phase was transferred and diluted to 4 mL. Then, the whole dispersion was subjected to 2 hr low frequency sonication (keeping the temperature constant) and centrifuged at 7000 rpm. Again, the supernatant phase was transferred to round bottom flask. The clear dispersion was drop cased on the precleaned mica sheet for AFM.

#### *1.5.2. HSA-PER@PDA-COF-1 preparation*

2 mg of PER@PDA-COF-1 was dispersed in 1 mL mili-Q water via bath sonication during 30 min. Then the solution was centrifuged at 4000 rpm and collected the supernatant solution.

Then the supernatant phase was transferred and diluted to 4 mL. Then, the whole aqueous dispersion was subjected to 1 hr low frequency sonication (keeping the temperature constant) and centrifuged at 7000 rpm. Again, the supernatant phase was transferred to round bottom flask. Then, HSA (10-30  $\mu$ L, 0.3 mM) was added to the faint yellow aqueous solution of PER@PDA-COF-1. The whole solution was vortexed for 60 min. Then the solution was centrifuged at 3000 rpm and the supernatant layer was discarded (to remove the unbounded HSA). The yellow mass was again dissolved in 2 ml water and sonicated for 2 h. Then the solution was drop casted for AFM.

### **1.6 Electrochemical Measurement**

Adsorption affinity of various Proteins (HSA, BSA, Concanavalin A, Cytochrome, Trypsin) on PER@PDA-COF-1 surface were examined by using CHI 760D electrochemical workstation in 0.1 M KCl solution as an electrolyte. Electrochemical analysis was carried out in three-electrode configuration with protein corona modified glass carbon electrode as working electrode, platinum as counter electrode, and Ag/AgCl as reference electrodes. Each sample was prepared by using same amount of COF adsorbed with same equivalent of proteins.

3 mg PER@PDA-COF-1 was suspended in 3 ml water and sonicated for 10 minutes. Then the suspended solution was divided into six portions. 50  $\mu$ L of 0.3 mM solution of various proteins (HSA, BSA, Concanavalin A, Cytochrome, Trypsin) was added to each portion and sonicated for 30 minutes. Then each solution was centrifuged at 8000 rpm and precipitate was collected for catalytic ink preparation. For ink preparation, the precipitate was redissolved in 200  $\mu$ L water and 5  $\mu$ L of Nafion solution (0.5 wt%) was added into it. Then, 30  $\mu$ L of each solution was drop casted on glassy working electrode (GCE) two times. After dried the (GCE) at 45 °C for 2 h, the working electrode was placed into electrolyte for measuring cyclic voltammetry (CV) between -1V and +1V at scan rate of 50 mV/s.

### **1. 7. Cell Culture**

Cultures of the cell line (HeLa) were maintained in Dulbecco's modified Eagle's medium (DMEM) containing 10% fetal bovine serum (FBS) and 1X pen strep (100 units/ml penicillin and 100 $\mu$ g/ml streptomycin). The cells were incubated at 37 °C under 5% CO<sub>2</sub> environment with relative humidity >95%. The cells were maintained by passaging 3-4 times a week using 0.5% trypsin-EDTA.

### **1. 8. Cell Cytotoxicity Assay**

Cytotoxicity of PER@PDA-COF-1, MXT-PER@PDA-COF-1 and HSA-MXT-PER@PDA-CON-1 were measured in HeLa cell line using MTT (3-(4,5-dimethylthiazol-2-yl)-2,5-diphenyl tetrazolium bromide) assay. Cells were seeded at a density of  $1 \times 10^4$  cells/well in a 96-well plate and after 24 h of incubation, various concentrations of mitoxantrone (10-70  $\mu\text{M}$ ), PER@PDA-COF-1 (0.2 mg/ml) were added to the cells in triplicate by the method of half dilution. After an incubation of 12, 24, 36 and 48 h, 20  $\mu\text{L}$  of MTT solution (5 mg/mL in 50 mM PBS, pH 7.4) was added to each well and further incubated at 37 °C for 3.5 h for complete settling of the formazan crystals. Thereafter the supernatant media were removed and 200  $\mu\text{L}$  of DMSO was added to each well to dissolve formazan. The absorbance of the DMSO solution was measured at a wavelength of 570 nm on a microwell plate reader (BioTek Epoch 2 Microplate Reader). The variation in cell viability with concentration was plotted using the obtained absorbance values. The % cell viability was calculated as:

$$\% \text{ Cell viability} = [(A_{590} \text{ Sample} - A_{590} \text{ DMSO}) / (A_{590} \text{ control} - A_{590} \text{ DMSO})] \times 100$$

### **1.9. Microscopy and determination of released mitoxantrone inside cells**

Cells were seeded at a density of  $5 \times 10^4$  cells/well in a 24 well plate and after 24 h of incubation, media were aspirated and new media were added in different wells. Dulbecco's modified Eagle's medium (DMEM) containing 10% Fetal Bovine Serum (FBS) and 1  $\times$  pen strep (100 units/mL penicillin and 100  $\mu\text{g}/\text{mL}$  streptomycin) were added to the cell culture wells. Mitoxantrone was added at a final concentration of 50  $\mu\text{M}$  adsorbed in PER@PDA-COF-1 (0.2 mg/mL). HSA was added to a final concentration of 350  $\mu\text{M}$  for making the corona complex with mitoxantrone adsorbed onto COF. Fluorescence microscopic images were taken using an Olympus CX81 fluorescence microscope. For the determination of release of mitoxantrone inside the cells, Radioimmunoprecipitation assay buffer (RIPA buffer) was added to culture wells and pipetted carefully to lyse the cells. These cell lysates were collected in different vials for centrifugation at 6000 rpm for 10 min. The cell debris were precipitated and the supernatants were collected for further fluorescence spectroscopic measurements for the released mitoxantrone at 600 nm. Cell lysates were prepared in a similar fashion for the ethidium bromide-acridine orange assay.

### **1.10. Determination of intracellular ROS generation**

Conjugated systems were investigated for probing the reactive oxygen species (ROS) generation inside cells. 1,3-Diphenylisobenzofuran (DPBF) was used to detect  ${}^1\text{O}_2$ . 1 mL of the cell lysates were taken from  $5 \times 10^4$  cells treated with MXT-PER@PDA-CON-1 and HSA-MXT-PER@PDA-CON-1 at different time points. 10  $\mu\text{L}$  (10 mM) DPBF solution was added

to the 1 mL cell lysate suspensions. The solution mixture was then irradiated with 635 nm laser for 15 min. Absorption intensity was measured at 420 nm. For control, the absorbance of water was measured. Comparative data were plotted at 1 h and 3 h time points.

### **1.11. Hemocompatibility**

Human blood was collected from unmedicated healthy volunteers and was stored in trisodium citrate (anti-coagulant) treated tubes. All the blood compatibility experiments were performed according to standard ISO protocol (10993-4). Experiments were carried out within 2 hours of blood collection. Hemocompatibility of PER@PDA-COF-1, MXT-PER@PDA-COF-1, HSA\_MXT-PER@PDA-COF-1 was evaluated by studying hemolysis, the morphology of blood cells, and coagulation activation, both through the extrinsic pathway (prothrombin time, PT assay) and the intrinsic pathway (activated partial thromboplastin time, APTT assay).

#### 1.11.1 Micrographs of blood smear:

After blood incubation with the systems, 10 µL of the blood was withdrawn and spread on a cleaned microscopy glass slide. Blood cells were observed with an Olympus CKX41 fluorescence microscope at 20× magnification in transmission mode.

#### 1.11.2. Clotting time

Whole human blood was used for determining the blood clot time. Collected blood was recalcified to reverse the effect of citrate anticoagulant and supplied with the specific activators of coagulation. Prothrombin time (PT) to evaluate the extrinsic pathway was carried out using thromboplastin reagent (Uniplastin from Tulip diagnostics), and activated partial thromboplastin time (APTT) to evaluate the intrinsic pathway was measured using cephaloplastin reagent (Liquicelin-e from Tulip diagnostics) as per kit protocol. For PT and APTT assay, plasma was isolated by centrifuging at 2000g for 5 minutes and the supernatant is used. In brief 50 µL of human plasma was incubated with samples (PER@PDA-COF-1, MXT-PER@PDA-COF-1, HSA\_MXT-PER@PDA-COF-1) on a cleaned glass slide. The very first visible sign of the clot was taken as the clotting of blood. PEI was used as a positive control and PBS served as the control experiment.

#### 1.11.3. Hemolysis assay

Whole blood was incubated with different concentrations of liposomes (PER@PDA-COF-1, MXT-PER@PDA-COF-1, HSA\_MXT-PER@PDA-COF-1), the samples were centrifuged at 600g for 5 minutes at room temperature, and supernatants were collected. The hemoglobin released was measured by the absorbance of 100-fold dilution of whole blood in Drabkin's

reagent at 540 nm in a microplate reader (Genetix epoch 2). A standard calibration curve was made using hemoglobin as the standard. PEI and PBS were used as positive and negative controls, respectively. The experiments were done in triplicate. The % of hemolysis was calculated by the relative method based on the Optical density (OD).

$$\% \text{ of hemolysis} = (\text{OD}_{\text{Sample}} - \text{OD}_{\text{Negative}}) / (\text{OD}_{\text{Positive}} - \text{OD}_{\text{Negative}}) \times 100.$$

## Section S2: Materials and Synthetic scheme

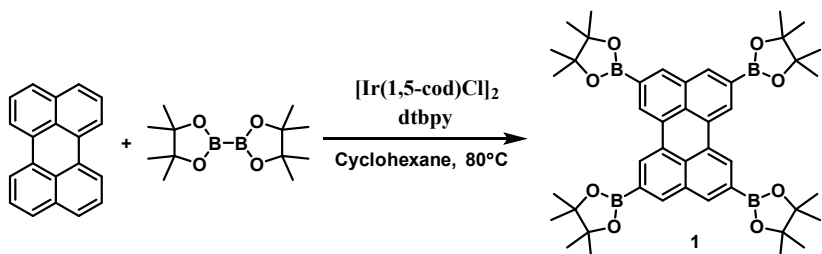
### 2.1. Materials

Perylene, Bis(1,5-cyclooctadiene)diiridium(I) dichloride, *p*-phenylenediamine and 4,4'-Di-tert-butyl-2,2'-dipyridyl were purchased from Aldrich, while bis(pinacolato)diboron, 4-bromo-benzaldehyde, tetrakis-(triphenylphosphine) palladium(0), were purchased from spectrochem, India. Dioxane, acetone, cyclohexane, o-dichlorobenzene, N,N' dimethyl acetamide etc. were purchased from Merck chemicals. These materials were used for synthesis without further purification.

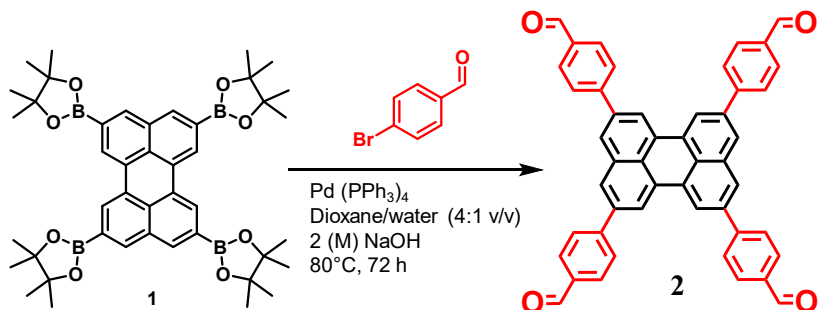
### 2.2. Synthetic scheme

#### 2.2.1. Synthesis of 2,5,8,11-tetrakis(4,4,5,5-tetramethyl-1,3,2-dioxaborolan-2-yl)perylene (P-bpin<sub>4</sub>) (1)

Perylene (0. 5 g, 1.98 mmol) and 3 g bis-(pinacolato)-diboron (11.88 mmol) were mixed together in anhydrous cyclohexane in a 50 mL Schlenk flask. Then 132 mg of [Ir(COD)OMe]<sub>2</sub> (10 mol%) and 40 mg of 4,4'-di-tert-butyl-2,2'-dipyridyl (10 mol%) were added to the solution under extremely inert condition (argon environment). Then the mixture was degassed with 5/6 consecutive freeze-pump-thaw cycles to exclude dissolved oxygen completely. The colour of the solution turned from yellow to green gradually which was further heated under reflux at 80°C for 72 hrs. During the reaction the flask was anchored by Al-foil to keep the mixture away from visible light. After reflux, the mixture was extracted with dichloromethane and the combined organic layer was evaporated off to get the crude product as a yellow semi-solid. The crude was further purified by silica gel column chromatography using DCM-ethyl-acetate (5:1) mixture to get the pure product as a bright yellow solid (1.3 g, 90 %).



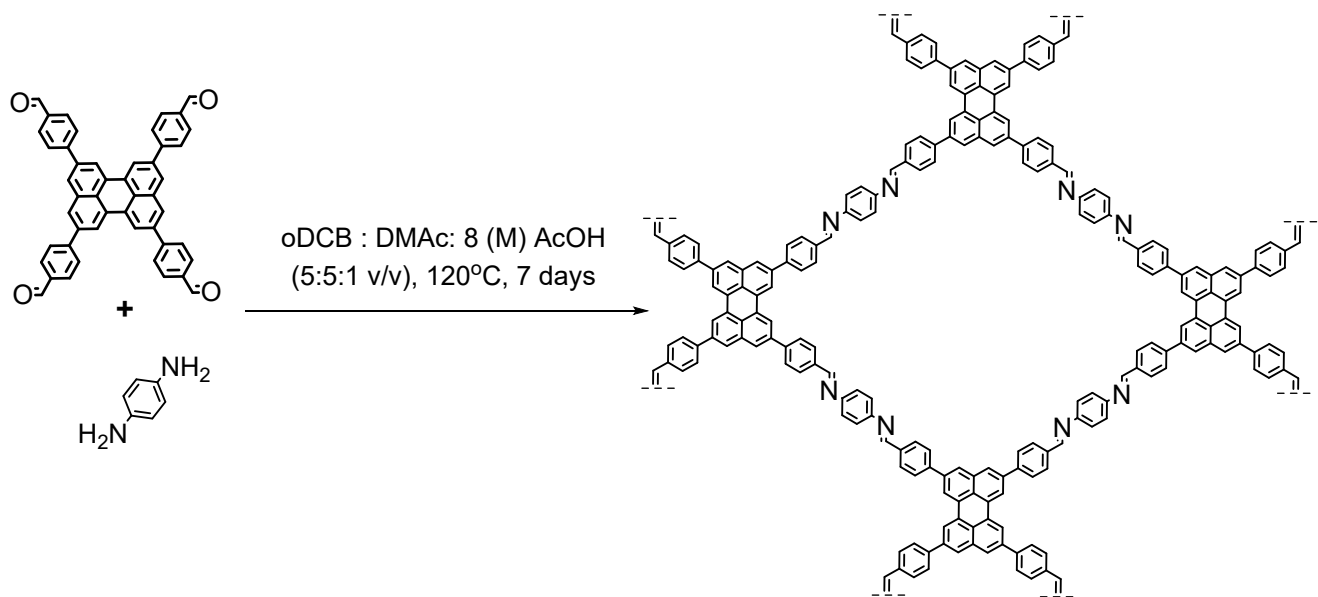
**2.2.2. Synthesis of 4,4',4'',4'''-(perylene-2,5,8,11-tetrayl) tetrabenzaldehyde (TFPPe) (2)**  
 Compound **1** 0.5 g (0.659 mmol) of and 0.731g (3.954 mmol) 4-bromobenzaldehyde were dissolved in 20 ml dioxane/aqueous 2M K<sub>2</sub>CO<sub>3</sub> mixture (4:1 v/v). Then 200 mg (5 mol%) Pd(PPh<sub>3</sub>)<sub>4</sub> was added to the mixture under N<sub>2</sub> atmosphere. The mixture was degassed by 3/4 consecutive freeze-thaw cycles and the mixture was refluxed at 80 °C for 3 days. The pure compound was obtained by simple filtration and successive washing with diethyl ether (5 x 100 mL) and was isolated as a deep orange solid TFPPe (0.4 g, 90 % yield). <sup>1</sup>H NMR (400 MHz, DMSO-d<sub>6</sub>): 10.14 (s, 4H, Ar H), 8.95 (s, 4H, Ar H), 8.39 (s, 4H, Ar H), 8.27 (d, 8H, J= 8 Hz, Ar H), 8.12 (d, 8H, J= 8 Hz, Ar H); IR (KBr):  $\nu$  (cm<sup>-1</sup>) = 2806 (w), 2722 (w), 1697 (s), 1595 (s), 1566 (w), 1435 (w), 1385 (w), 1339 (w), 1308 (w), 1216 (m), 1172 (m), 1109 (w), 1013 (w), 884 (m), 824 (s), 734 (w). Calculated C, H, N analysis for C<sub>48</sub>H<sub>28</sub>O<sub>4</sub>: C 86.21, H 4.22; found: C 86.31, H 4.27%. Mp > 300°C.



### 2.2.3. Synthesis of 2D PER@PDA-COF-1

A glass seal tube (20 cm x 8 mm) was charged with 33 mg of TFPPe (**2**, 50 μmol) and 10 mg (100 μmol) of p-phenylenediamine (**3**). The solid mixture was dissolved in DMAc/o-DCB (1:1 v/v, 1 ml) using 100 μL 8 (M) acetic acid. The mixture was sonicated for 5 min and frozen in

a liquid N<sub>2</sub> bath and degassed through 3/4 freeze-pump-thaw cycles and flame sealed under vacuum which was kept inside oven for 7 days under static heating at 120 °C. The PER@PDA-COF-1 material was obtained as a yellowish-orange insoluble powder which was activated by repeated washing with THF, acetone, water and methanol, n-hexane (25 mg, yield 58%). C, H, N calculated: C 90.93, H 4.99, N 4.08; found: C 91.2, H 5.5, N 3.8 %.



#### 2.2.4. <sup>1</sup>H NMR spectra

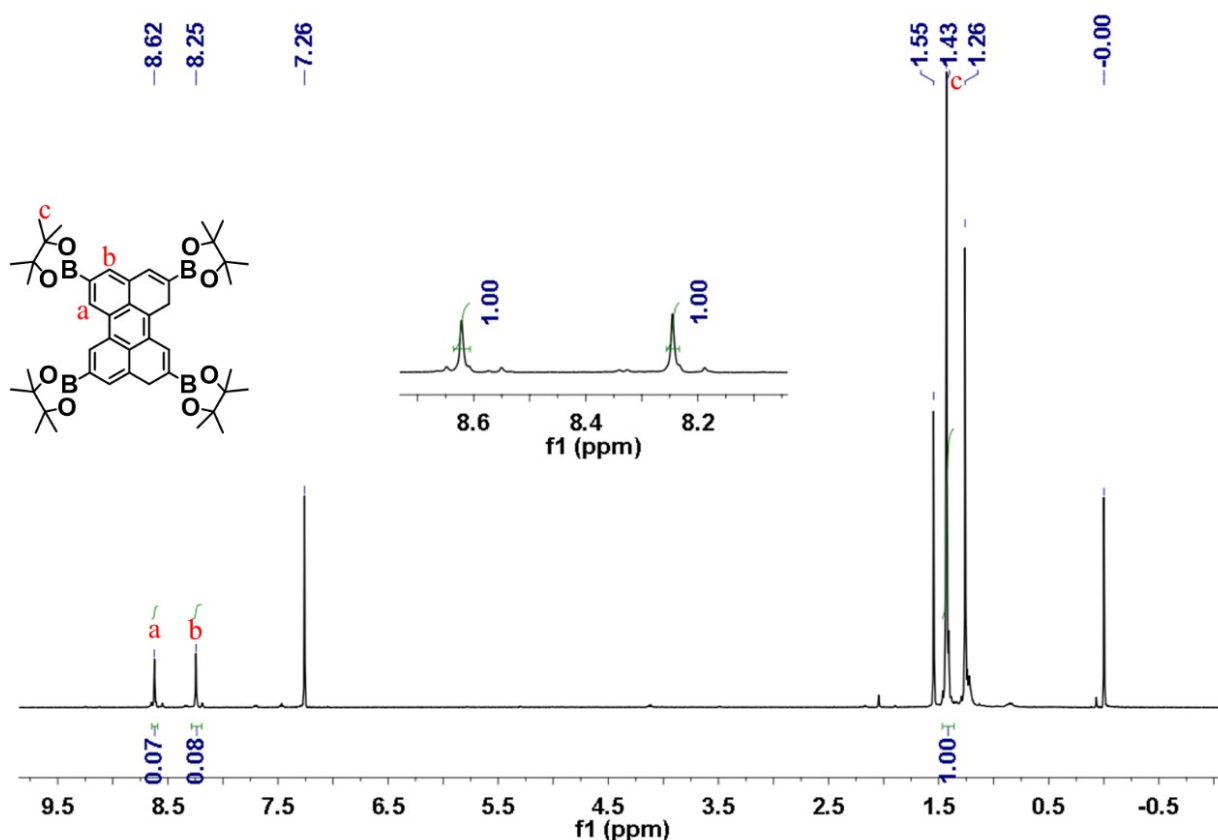


**Figure S1.**  $^1\text{H}$ -NMR (in  $\text{CDCl}_3$ ) spectrum of 2,5,8,11-tetrakis(4,4,5,5-tetramethyl-1,3,2-dioxaborolan-2-yl)perylene ( $\text{P-bpin}_4$ )

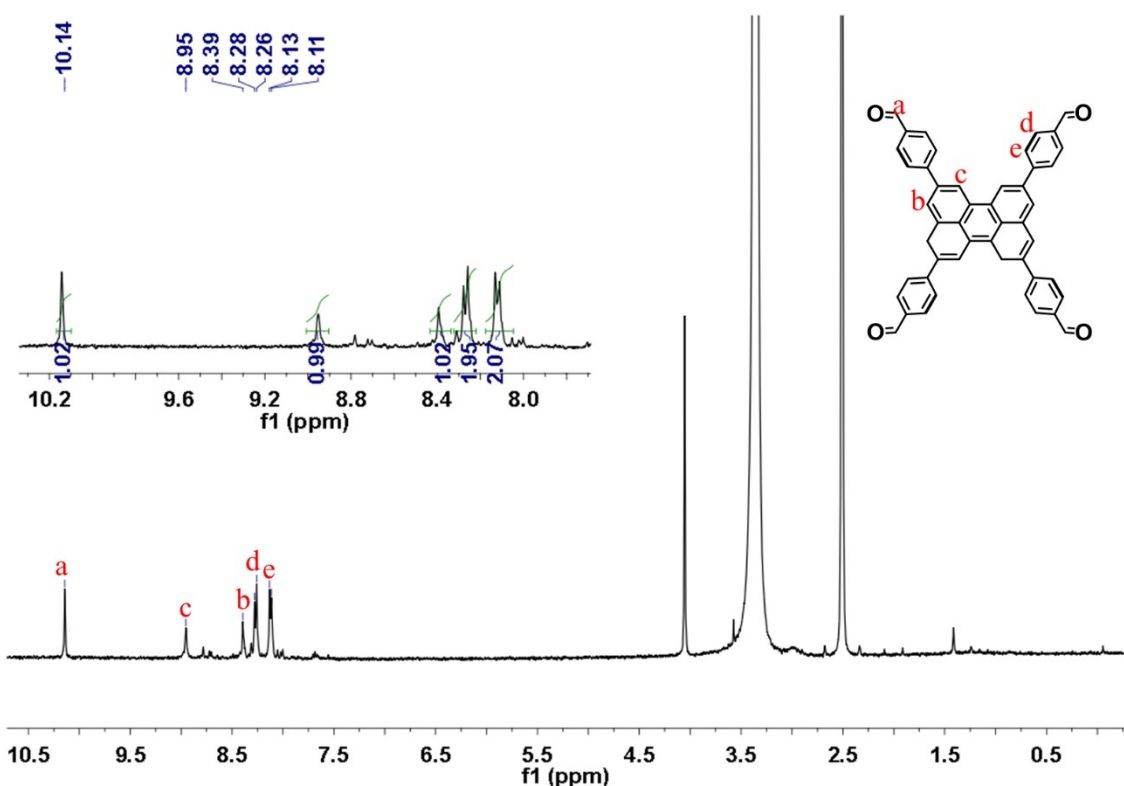


**Figure S2.**  $^1\text{H}$  NMR (in  $\text{D}_6\text{-DMSO}$ ) spectrum of 2,5,8,11-tetrakis(4-formylphenyl) perylene (TFPPe) (note that  $^{13}\text{C}$  NMR spectra could not be recorded due to low solubility of TFPPe).

### Section S3: Computational Details

The crystalline structure of PER@PDA-COF-1 was determined by building square lattice (**sql**) and kagome (**kgm**) structures using AuToGraFS.<sup>1</sup> Structures were optimized using the density-functional tight-binding (DFTB+) method as implemented in DFTB+ program package version 1.3.<sup>2</sup> The Coulombic interaction between partial atomic charges was determined using

















H69	0.79003	0.22058	0.0512	H141	0.41331	0.5997	0.46037	H213	0.64983	0.74577	0.56762
C119	0.71468	0.24539	0.06558	C238	0.34815	0.49994	0.48781	C359	0.57401	0.79476	0.55071
H70	0.69514	0.2166	0.07942	H142	0.32511	0.51968	0.45888	H214	0.55293	0.84362	0.54375
H71	0.74083	0.26808	0.06239	C239	0.54002	0.16403	0.41551	H215	0.60144	0.74614	0.57142
N8	0.68655	0.27161	0.07801	H143	0.55652	0.16251	0.29151	N24	0.54728	0.79388	0.55614
C120	0.67933	0.29418	0.95458	C240	0.66132	0.01039	0.46709	C360	0.52516	0.8099	0.43077
H72	0.69455	0.29374	0.82421	H144	0.64596	0.01083	0.33817	H216	0.52632	0.82465	0.30322

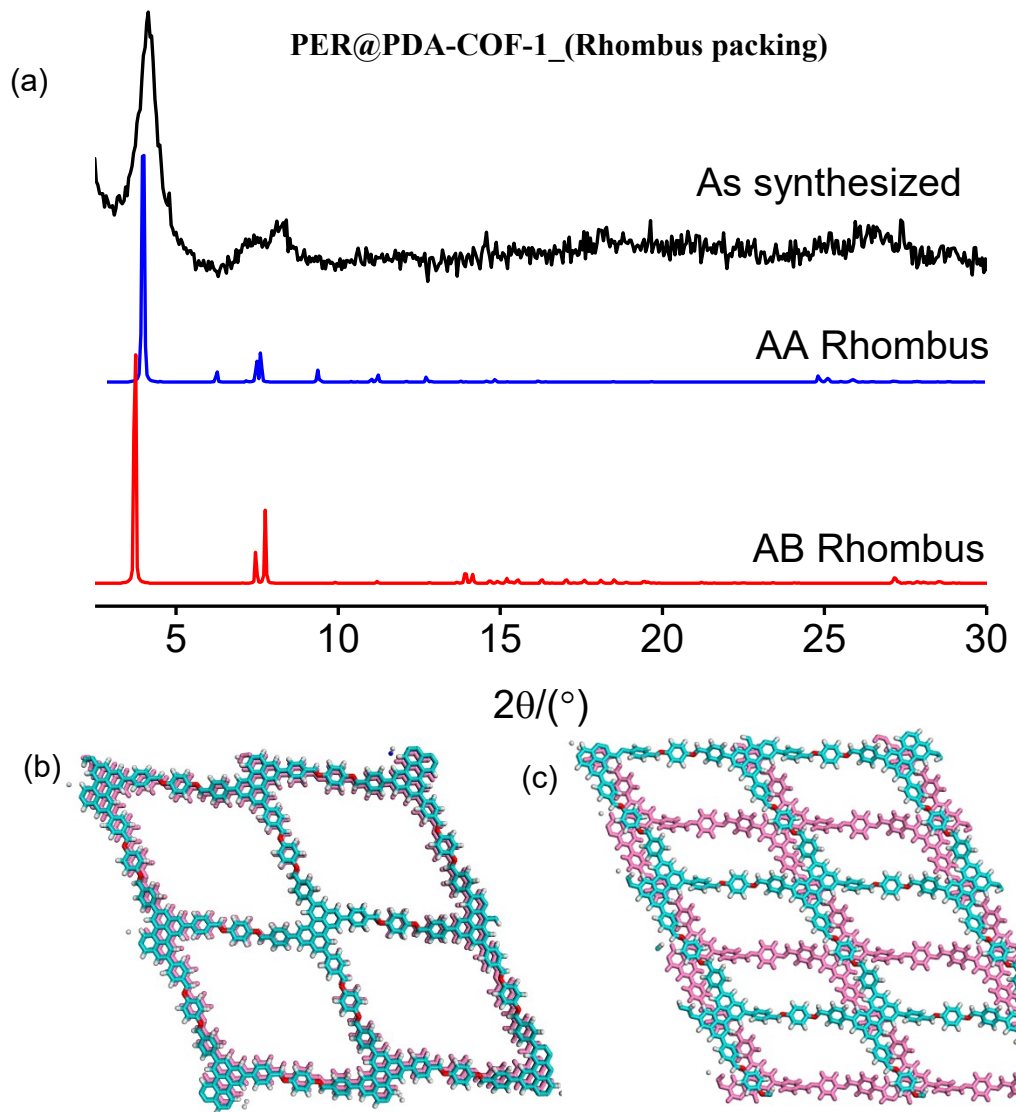


**Figure S3.** (a) Experimental powder X-ray diffraction pattern (PXRD) of PER@PDA-COF-1 (black plot), theoretical PXRD pattern for eclipse (AA) stacking of rhombus net of PER@PDA-COF-1 (blue plot) and Staggered (AB) stacking of rhombus net of PER@PDA-COF-1 (red plot); (b) Atomistic model of AA stacking of rhombus PER@PDA-COF-1 structure; (c) Atomistic model of AB stacking of rhombus PER@PDA-COF-1 structure.

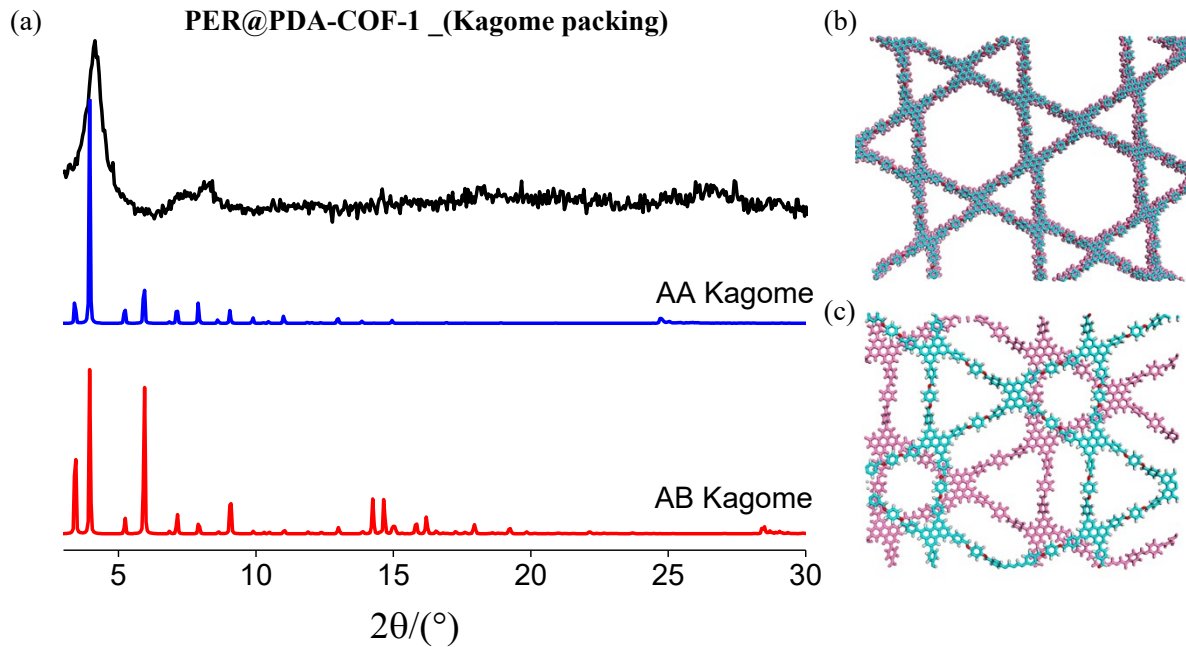


**Figure S4.** (a) Experimental powder X-ray diffraction pattern (PXRD) of PER@PDA-COF-1 (black plot), theoretical PXRD pattern for eclipse (AA) stacking of kagome net of PER@PDA-COF-1 (blue plot) and Staggered (AB) stacking of kagome net of PER@PDA-COF-1 (red plot); (b) Atomistic model of AA stacking of kagome PER@PDA-COF-1 structure; (c) Atomistic model of AB stacking of kagome PER@PDA-COF-1 structure.

Rhombus_PER@PDA-COF-1_AA + Mitoxantrone (Space group - P1) $a = 25.6974 \text{ \AA}$ , $b = 26.1652 \text{ \AA}$ , $c = 20.000 \text{ \AA}$ ; $\alpha = 90^\circ$ , $\beta = 90^\circ$ , $\gamma = 110^\circ$											
<i>Atom</i>	<i>x</i>	<i>y</i>	<i>z</i>	<i>Atom</i>	<i>x</i>	<i>y</i>	<i>z</i>	<i>Atom</i>	<i>x</i>	<i>y</i>	<i>z</i>
C1	0.4774	0.67776	0.95252	C37	0.67232	0.07893	0.99676	C68	0.62913	0.73727	0.82297
C2	0.53208	0.67668	0.95957	H18	0.71959	0.02834	0.02401	C69	0.60134	0.77725	0.82284
C3	0.57741	0.72647	0.96763	C38	0.62295	0.08193	0.96945	C70	0.5419	0.75989	0.81784
C4	0.56682	0.77669	0.97085	H19	0.54372	0.03421	0.92537	C71	0.51511	0.79924	0.8242
C5	0.51219	0.77559	0.96662	H20	0.70382	0.11638	0.01497	C72	0.5474	0.85501	0.83519
C6	0.446704	0.72651	0.95704	C39	0.41045	0.72856	0.95082	C73	0.60421	0.87197	0.83605
C7	0.63238	0.72483	0.97194	C40	0.39488	0.76717	0.98721	C74	0.63251	0.83389	0.82893
C8	0.61355	0.82783	0.97744	C41	0.37151	0.6937	0.90676	H37	0.50916	0.52348	0.80989
C9	0.66861	0.82619	0.9796	C42	0.34262	0.77131	0.97946	H38	0.61236	0.55368	0.82179
C10	0.67927	0.77606	0.97598	H21	0.42427	0.79411	0.02263	H39	0.52691	0.88513	0.84226
C11	0.71418	0.87608	0.98467	C43	0.31943	0.69833	0.89839	H40	0.62816	0.91509	0.84371





N3	0.2138	0.80415	0.0309	H75	0.00334	0.38851	0.06808	H117	0.11334	0.86268	0.16227
N4	0.32827	0.70192	0.04696	H76	0.08597	0.35303	0.95661	H118	0.07489	0.8744	0.14963
C57	0.05053	0.28844	0.00233	C127	0.04178	0.40432	0.01148	C196	0.08688	0.87819	0.25247
H33	0.07012	0.27134	0.97294	C128	0.06718	0.40716	0.00928	H119	0.09086	0.85568	0.26692
C58	0.02184	0.16302	0.00623	C129	0.01333	0.43061	0.0117	H120	0.06343	0.89434	0.26685
H34	0.99934	0.18139	0.98984	C130	0.0649	0.43573	0.0087	C197	0.94788	0.01547	0.18107
C59	0.20898	0.82997	0.01096	H77	0.08951	0.38721	0.0091	H121	0.94647	0.99672	0.15792
H35	0.22723	0.8334	0.99039	C131	0.01004	0.45913	0.01025	H122	0.9303	0.0363	0.1576
C60	0.33435	0.67632	0.02271	H78	0.9935	0.42805	0.01194	C198	0.94316	0.01633	0.25631
H36	0.31745	0.67339	0.99352	C132	0.03614	0.46206	0.00991	H123	0.96084	0.99518	0.2787
C61	0.36364	0.64936	0.02937	C133	0.09103	0.43824	0.0067	H124	0.92131	0.01775	0.26685
C62	0.36806	0.62259	0.00046	C134	0.98054	0.48619	0.00921	N15	0.94379	0.04208	0.28441
C63	0.38789	0.64899	0.06246	C135	0.03424	0.49066	0.0106	H125	0.95509	0.04898	0.25293
C64	0.39567	0.59651	0.00359	C136	0.08914	0.4661	0.00552	N16	0.1079	0.88496	0.28578
H37	0.34938	0.62247	0.97455	H79	0.11288	0.41771	0.00467	H126	0.11594	0.89463	0.25246
C65	0.41561	0.62293	0.06501	C137	0.97863	0.51476	0.01295	C199	0.95706	0.0367	0.35095
H38	0.38475	0.66957	0.08592	C138	0.95427	0.48483	0.00491	H127	0.95161	0.05855	0.37322
C66	0.42013	0.59624	0.03532	C139	0.00475	0.51767	0.01448	H128	0.94685	0.02684	0.38311
H39	0.39849	0.57617	0.97955	C140	0.06049	0.4921	0.00779	C200	0.99079	0.01642	0.34937
H40	0.4342	0.62315	0.09106	C141	0.1163	0.46874	0.00198	H129	0.00054	0.02213	0.30576
C67	0.44977	0.56882	0.03519	C142	0.94989	0.5411	0.0149	H130	0.00109	0.01943	0.39556
C68	0.47586	0.57045	0.03427	C143	0.92565	0.51085	0.00662	C201	0.09607	0.90375	0.34482
C69	0.45207	0.54029	0.03323	H80	0.95542	0.46309	0.0012	H131	0.11492	0.90278	0.37362
C70	0.50433	0.54415	0.03094	C144	0.00148	0.54613	0.01926	H132	0.08521	0.89473	0.37757
H41	0.47469	0.59226	0.03438	H81	0.05927	0.51391	0.00822	C202	0.07395	0.93595	0.3264
C71	0.47958	0.51385	0.03035	C145	0.1156	0.49368	0.97162	H133	0.08532	0.94697	0.30207
H42	0.43137	0.5393	0.03478	C146	0.14368	0.44635	0.02848	H134	0.05679	0.93733	0.29115
C72	0.50641	0.51552	0.02963	C147	0.92374	0.53862	0.01246	O5	0.05829	0.95264	0.3857
				C148	0.94764	0.56961	0.01895	H135	0.07305	0.94963	0.41998
				C149	0.89844	0.50831	0.00233	O6	0.99815	0.98557	0.34489
				C150	0.97306	0.57242	0.02147	H136	0.01921	0.97293	0.35842

### Molecular dynamics simulation

Molecular dynamics was undertaken for a total of 500ps using a model of PER@PDA-COF-1 as follows: From the lowest energy rhombus AA structure (a bilayer), a 1x1x4 supercell was created, resulting in an 8-layer model COF containing 800 atoms. As the MXT molecule will only interact with some of those layers, the top four layers had their coordinates frozen. The four remaining layers were entirely unconstrained. The MXT molecule was added to the pore near the unconstrained layers. After 100ps of equilibration, 500ps of MD was undertaken in the NVT ensemble using a timestep of 0.25 fs. A Nose-Hoover chain thermostat was used to maintain a temperature of 300K.

Snapshots were extracted every 10000 steps and the binding energy of MXT-PER@PDA-COF-1 was calculated using Density Functional Tight Binding (DFTB). All atoms were described using the 3ob-3-1 parameter set with D3-BJ dispersion.

All calculations were undertaken using AMS 2022.101. Analysis was undertaken using VMD and a self-written python script. Using cutoffs of 3.5 Å for D-A distance and 140° for the hydrogen bond angle, on average one hydrogen bond was maintained between the MXT molecule and the PDA-COF-1. The most frequent hydrogen bond donors were the MXT amine groups.

Extending the definition to include all close contacts, rather than just hydrogen bonds involving polar atoms, showed an average of 26 MXT—PER@PDA-COF-1 contacts maintained throughout the trajectory, indicating that less specific intermolecular interactions dominate over hydrogen bonding. Supporting this, the average DFTB MXT@ PDA-COF-1 binding energy over the trajectory was 145 kJ/mol.

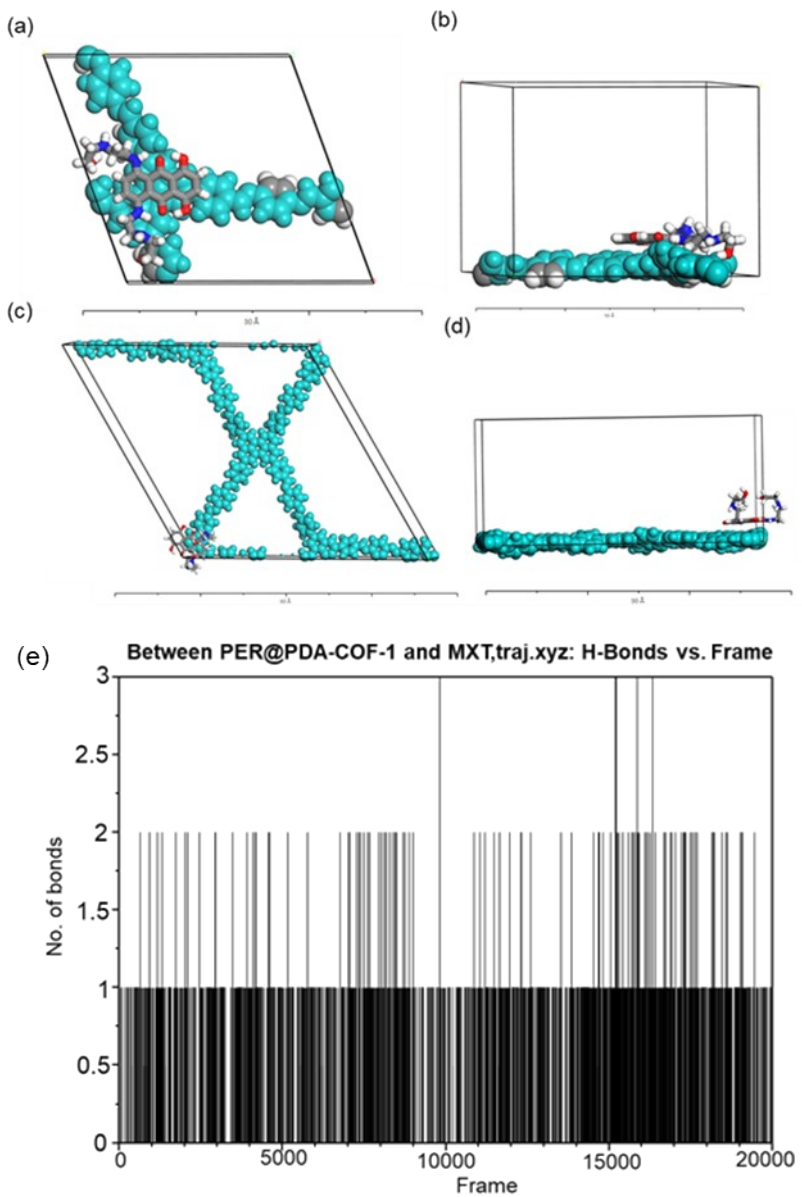


**Figure S5.** (a) Top view of the unit cell for MXT-PER@PDA-COF-1; (b) Side view of the unit for MXT-PER@PDA-COF-1 (Rhombus lattice); (c) Top view of the unit cell for MXT-PER@PDA-COF-1; (b) Side view of the unit for MXT-PER@PDA-COF-1 (Kagome lattice). where PER@PDA-COF-1 is depicted as cyan colour and the MXT molecule (Carbon in grey colour, Nitrogen in red colour, Hydrogen in white colour); (e) Number of hydrogen bond involved in the MXT-PER@PDA-COF-1 system with 200 ns time frame

## Section S4: FT-IR spectra

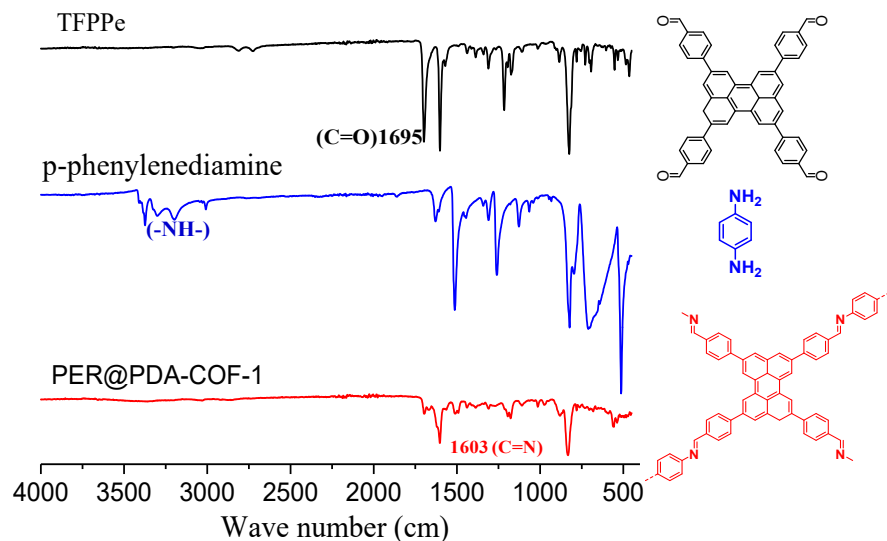


**Figure S6.** FTIR spectra of 4,4',4'',4'''-(perylene-2,5,8,11-tetrayl) tetrabenzaldehyde (TFPPe, black plot), p-Phenylenediamine (blue plot) and PER@PDA-COF-1 (red plot).

## Section S5: Solid state <sup>13</sup>C CP/MAS NMR

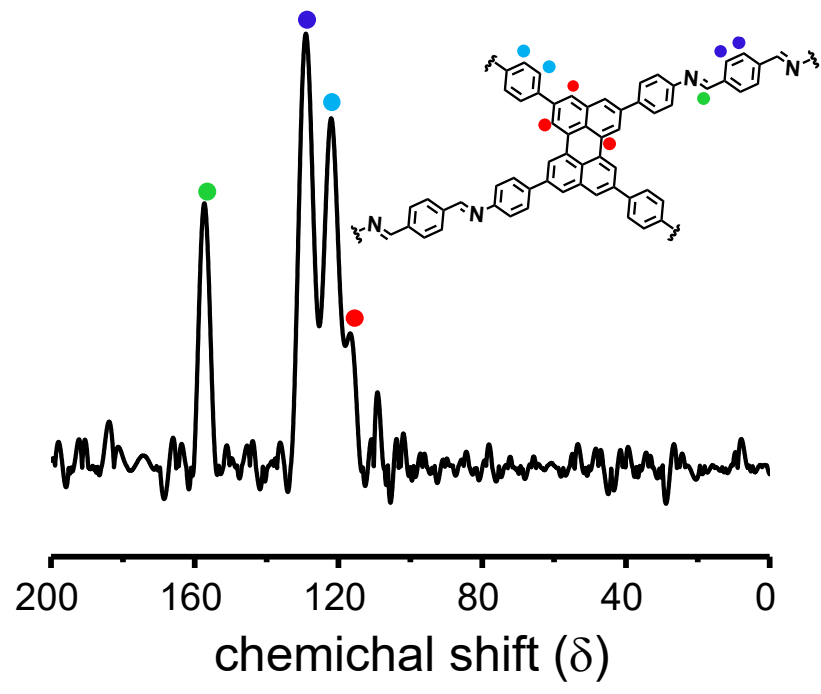


**Figure S7.**  $^{13}\text{C}$  solid state CP/MAS NMR of PER@PDA-COF-1

### Section S6: Thermo-gravimetric (TGA) analysis

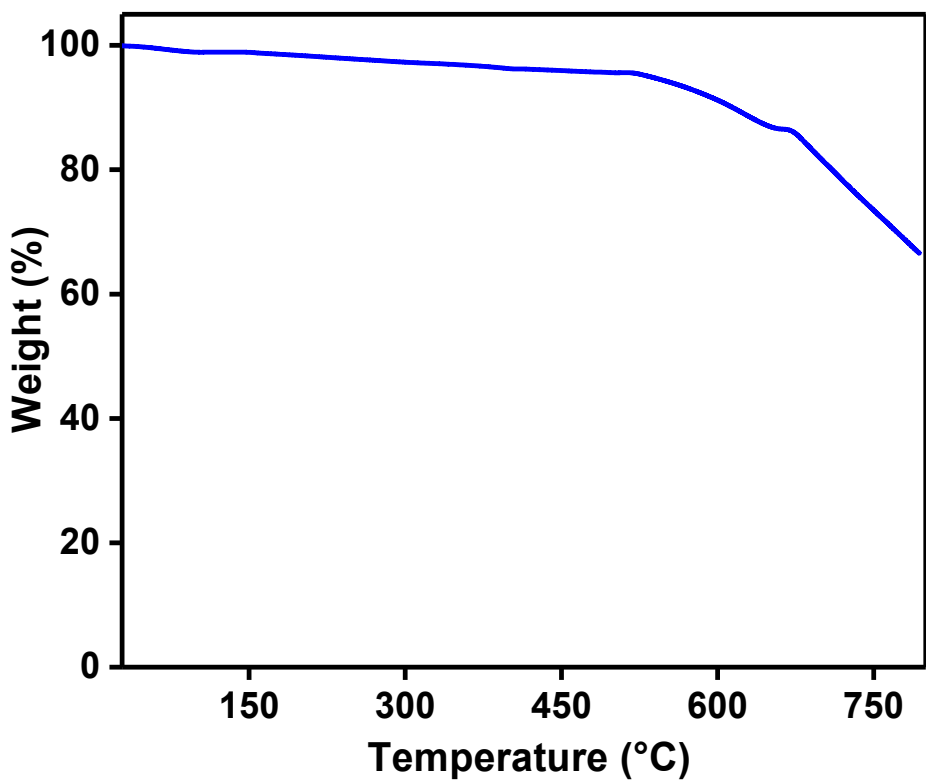


**Figure S8.** TGA plot of PER@PDA-COF-1 under  $\text{N}_2$

**Section S7: Ultra-high resolution transmission electron microscopy (UHR-TEM) analysis**

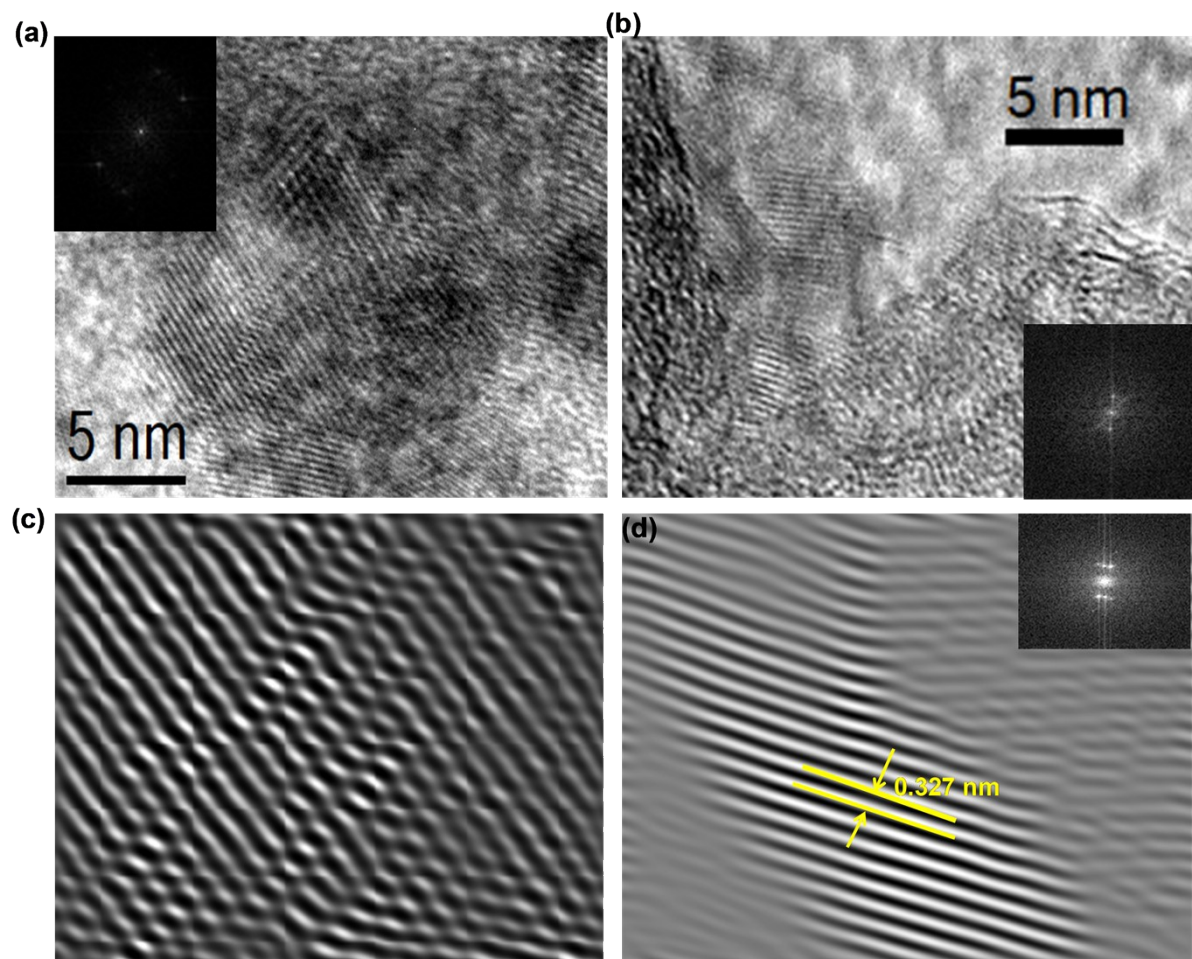


**Figure S9.** UHR-TEM image of the crystalline domain (a),(b) and the FFT pattern (inset); (c) Inverse FFT pattern; (d) distance between the two successive layers of the crystallite.

## Section S8: FT-IR spectra of Mitoxantrone (MXT) and MXT loaded COF

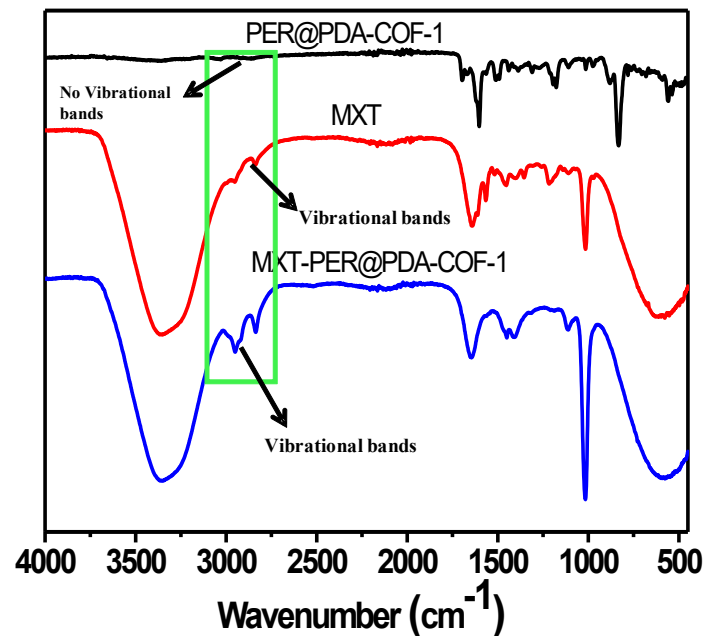


**Figure S10.** FTIR spectra of PER@PDA-COF-1 (black), MXT only (red) and MXT-PER@PDA-COF-1 (blue).

## Section S9: Change of absorption of MXT upon binding with PER@PDA-COF-1

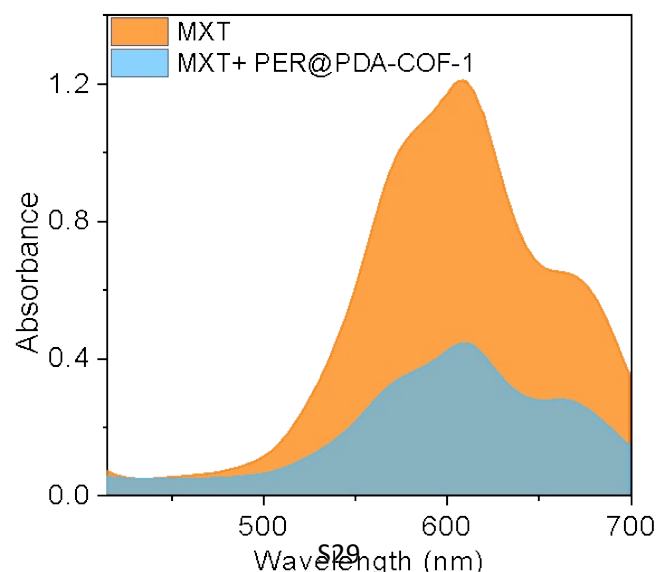


**Figure S11.** UV-Vis spectra of MXT before (orange) and after immobilization (blue) inside PER@PDA-COF-1.

### Section S10: Change of fluorescent spectra of COF upon binding with MXT and the linear regression plot

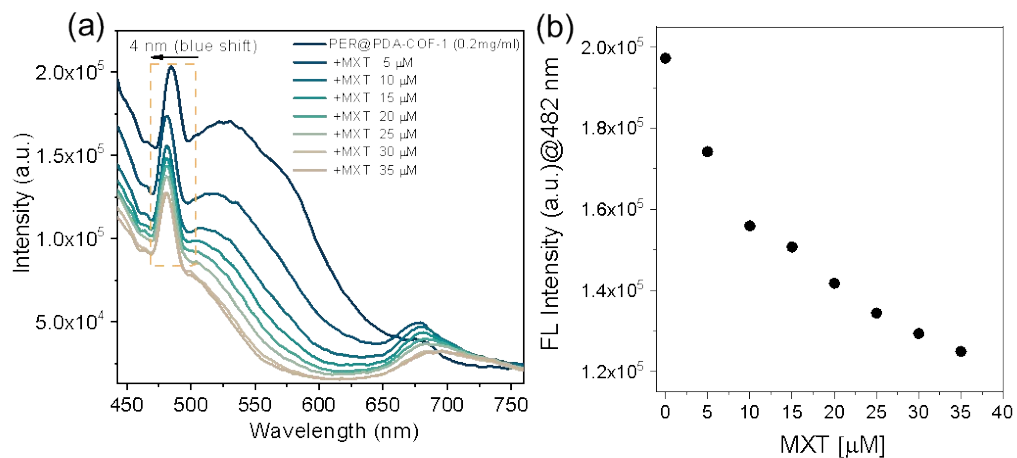


**Figure S12.** (a) Quenching of fluorescence emission of PER@PDA-COF-1 upon binding with mitoxantrone and (b) linear decrease in emission PER@PDA-COF-1.

### Section S11: Binding constant calculation ( $K_{sv}$ ) for the MXT binding with COF

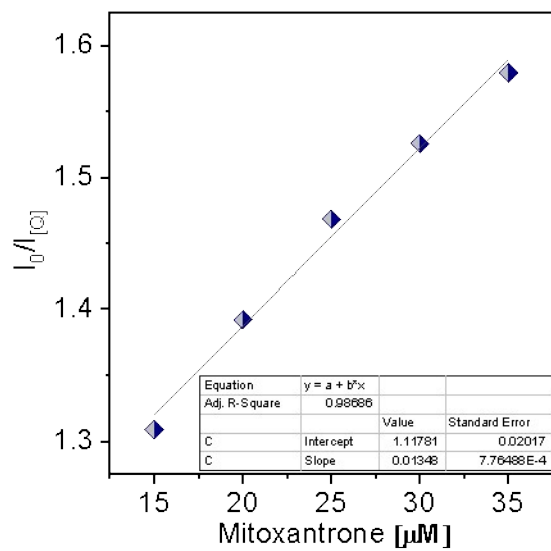


**Figure S13.**  $K_{sv}$  plot of MXT-PER@PDA-COF-1.

### Section S12: Job's plot analysis of binding of proteins

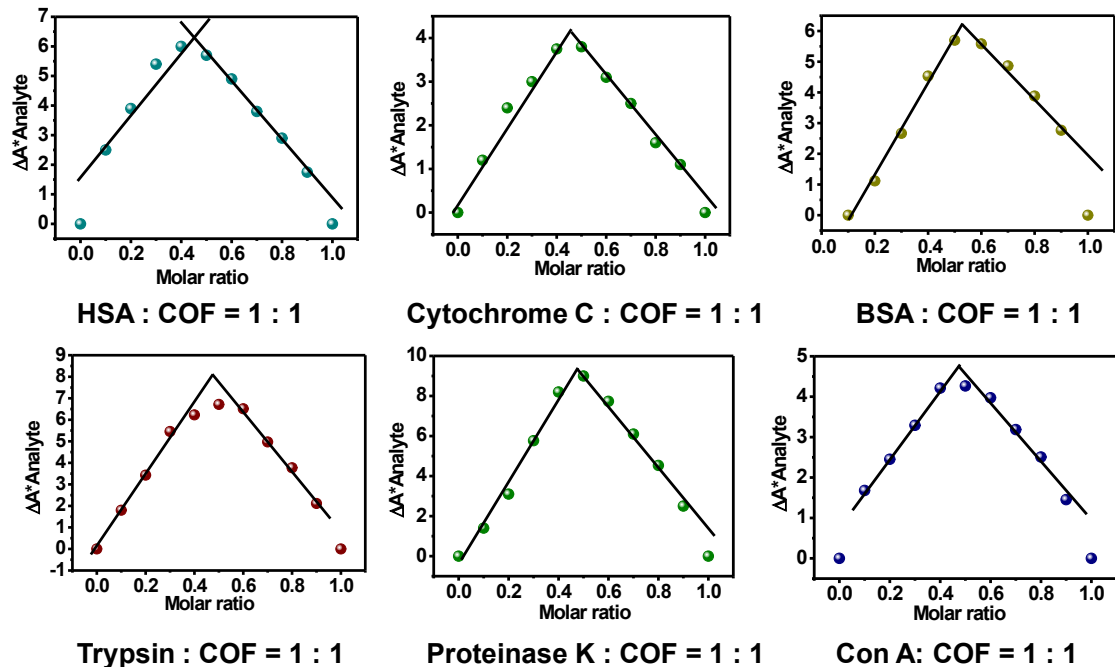


**Figure S14.** Job's plot analysis of binding of towards different proteins with the PER@PDA-COF-1 (COF).

### Section S13: Comparative study of the “Turn-ON” response of PER@PDA-COF-1 towards various proteins

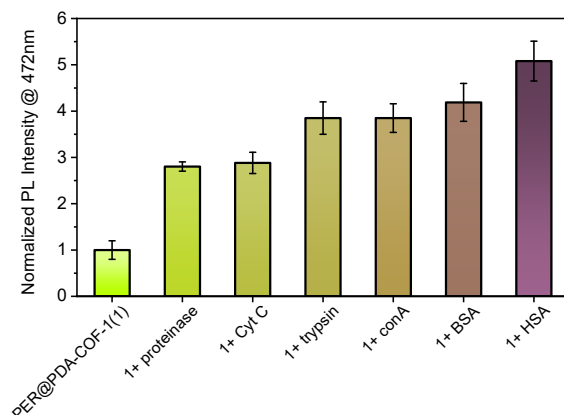


**Figure S15.** Turn-ON response of PER@PDA-COF-1 towards various proteins (Cyt C represents Cytochrome C, con A represents concanavalin A, BSA represents bovine serum albumin and HSA represents human serum albumin).

### Section S14: Cyclic voltammetry

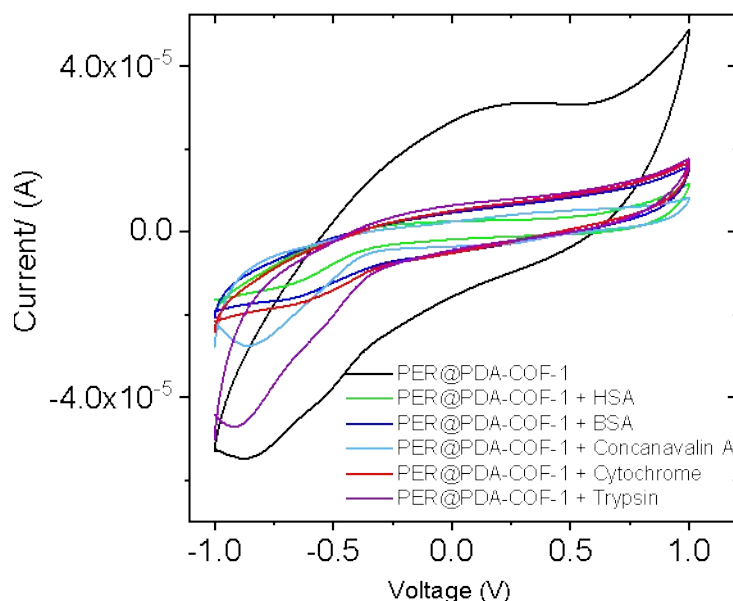


**Figure S16.** Cyclic voltammetry study of PER@PDA-COF-1 (black) only and the protein corona using HSA (green), BSA (blue), Concanavalin A (cyan), Cytochrome (red) and trypsin (purple).

### Section S15: Effect of urea and temperature on the stability of albumin/COF nano assembly

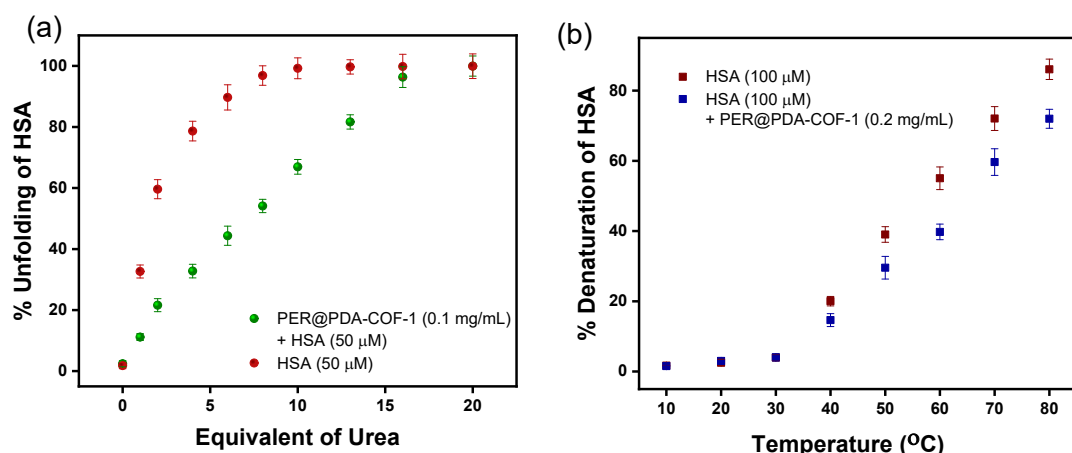


**Figure S17.** (a) Urea and (b) temperature dependent stability of albumin/COF nano-assembly.

**Section S16: Effect of pH on the stability of of albumin/COF nano assembly**

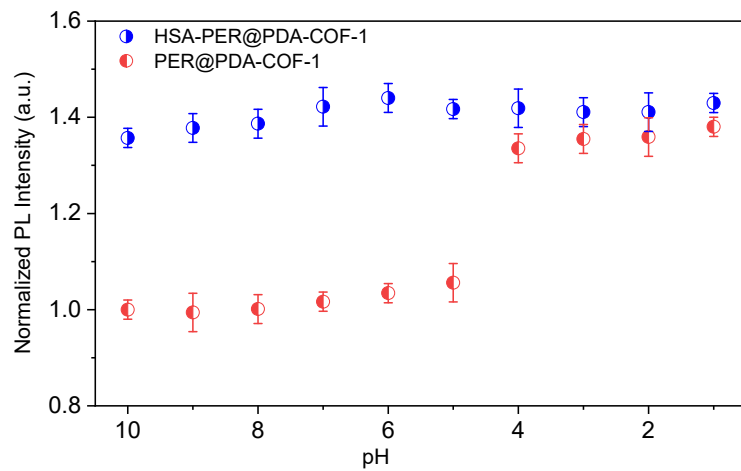


**Figure S18.** pH dependent stability of albumin/COF nano-assembly.

**Section S17: Effect of temperature and urea on MXT release by system I, system II and system III.**

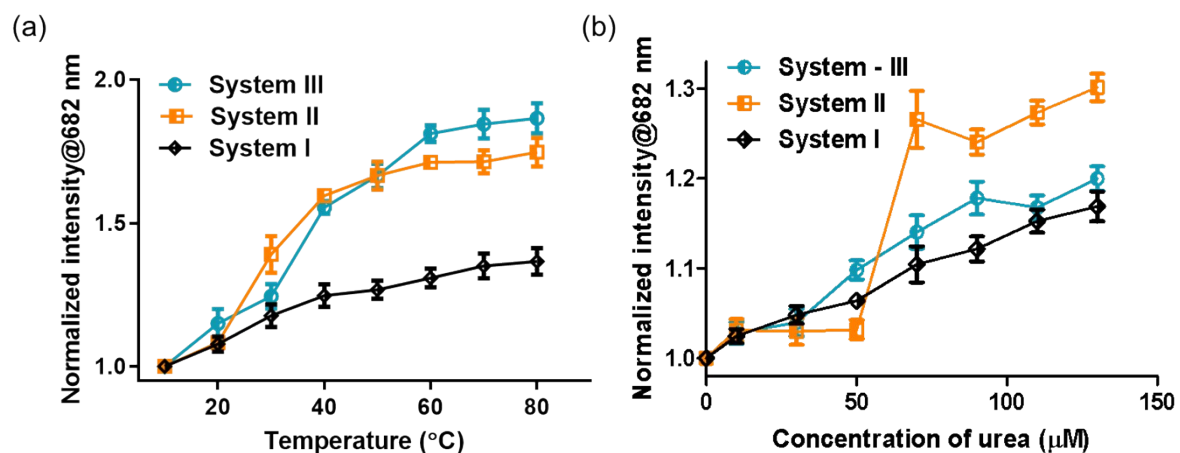


**Figure S19.** (a) Effect of temperature on release of Mitoxantrone release; (b) effect of urea concentration on MXT release from system-I, system-II & system-III.

### Section S18: Comparison of Proteinase-K stability of System-II and System-III

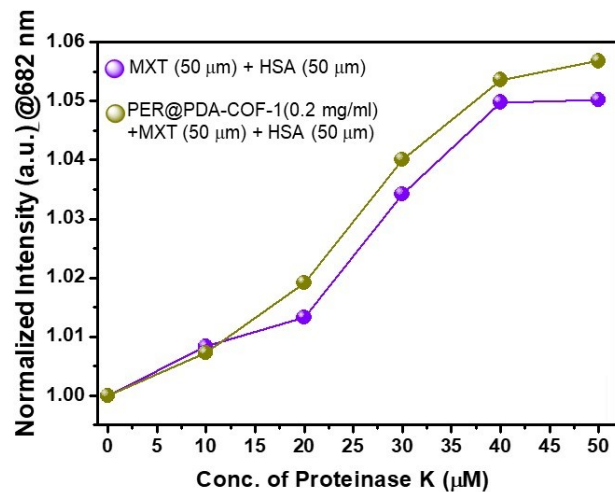


**Figure S20.** Proteinase-K stability of HSA-MXT-PER@PDA-CON-1.

### Section S19: Comparative time dependent cellular release profile of MXT from system-I, system-II, system-III and MXT only

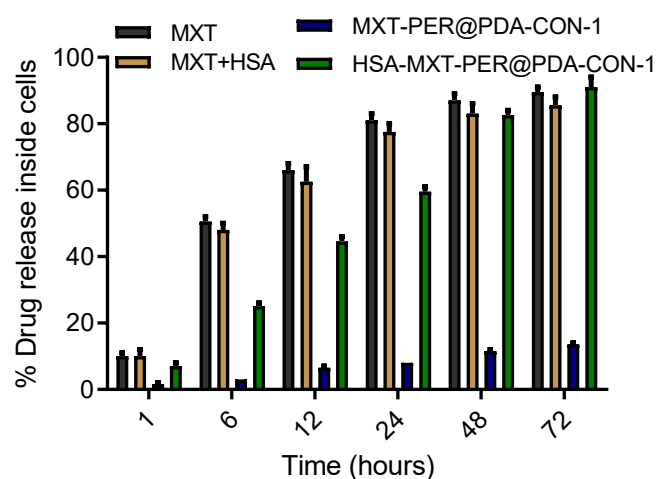


**Figure S21.** Comparative time dependent drug release studies among the different systems

**Section S20: Extracellular and intracellular distribution of Time dependent released MXT by MXT-PER@PDA-COF and HSA-PER@PDA-COF-1.**

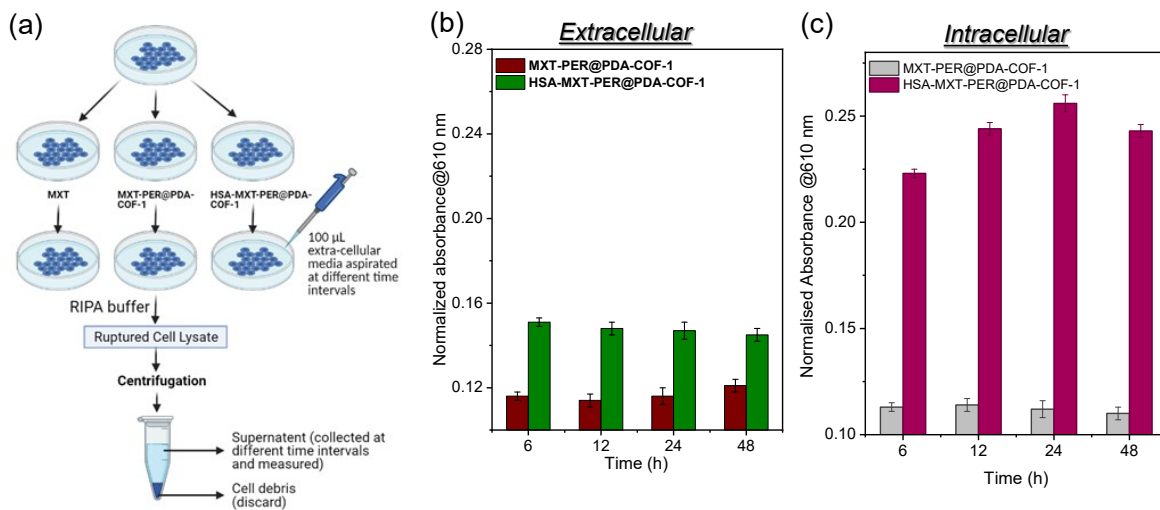


**Figure S22.** (a) Schematic demonstration for estimation of released MXT in extracellular and intracellular environment at different time interval; Comparison of (b) Extracellular and (c) intracellular release of MXT by MXT-PER@PDA-COF and HSA-PER@PDA-COF-1. The study was conducted using CT-26 cell line.

**Section S21: Fluorescent microscopy study of cellular internalization of MXT.**

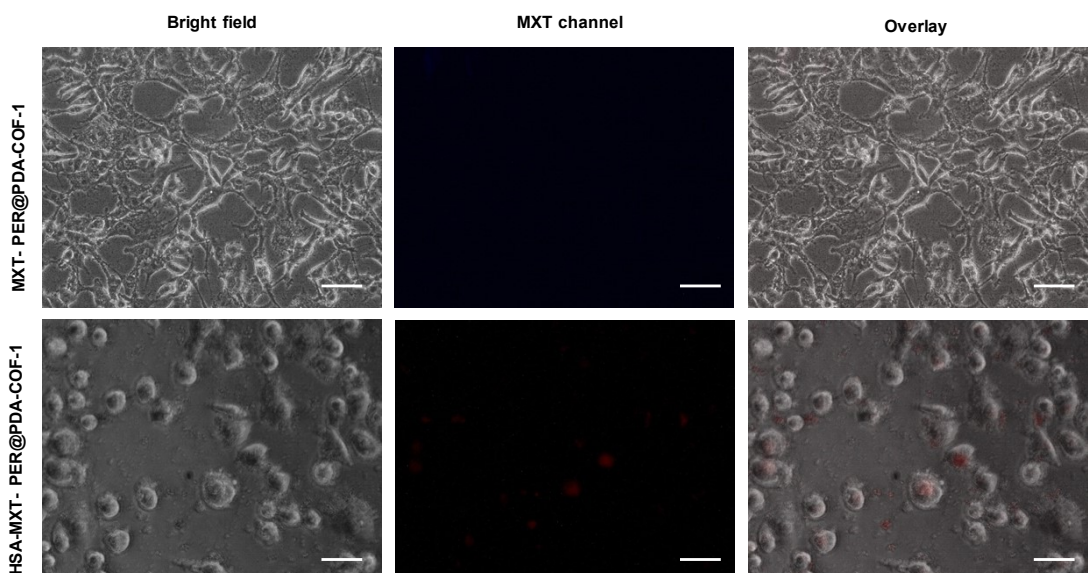


**Figure S23.** Comparative internalization of MXT inside cells (scale bar indicates 200  $\mu$ m)

**Section S22: Visualization of extracellular and intracellular MXT (CT-26 cell line).**

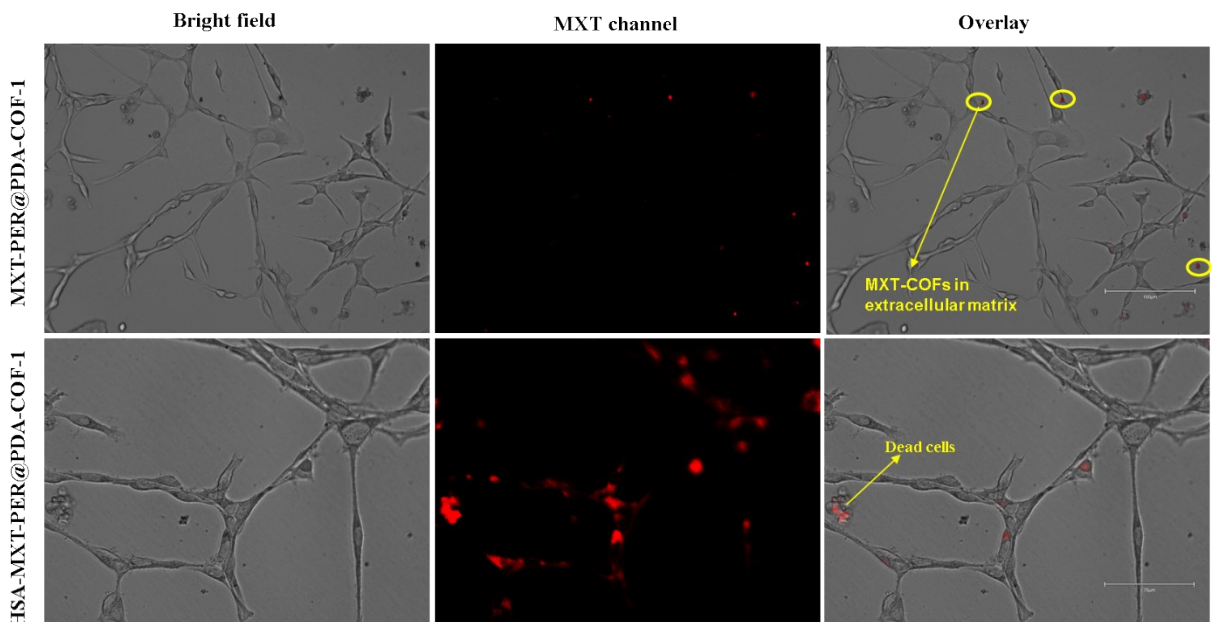


**Figure S24.** HSA induced improved internalization of MXT inside cells (scale bar indicates 200  $\mu$ m)

(a)

Compounds	Percentage of hemolysis
Normal Saline (Negative control)	0
TritonX (Positive control)	100
PER@PDA-COF-1	1.9%
MXT-PER@PDA-COF-1	1.7%
HSA_MXT-PER@PDA-COF-1	0.9%

(b)

Compounds	Clotting time (min)
Normal Saline (Negative control)	6 mins
PEI (Positive control)	30 seconds
PER@PDA-COF-1	5.2 mins
MXT-PER@PDA-COF-1	5.5 mins
HSA-MXT-PER@PDA-COF-1	5.6 mins

**Table S1.** (a) Comparative percentage of hemolysis; (b) clotting time using different biosystem along with system I, system II and PER@PDA-COF-1 only. (% hemolysis was negligible and blood clotting time was not affected)

### **Section S23: Mice tumor Models and *In vivo* Studies.**

The murine colon carcinoma cell line CT26 was purchased from ATCC and cultured in RPMI 1640 (Gibco) supplemented with 10% fetal bovine serum (Himedia) at 37 °C in a humidified atmosphere containing 5% CO<sub>2</sub> and 95% humidity. All Balb/c mice were maintained under the environment, providing sterilized food pellets and distilled water throughout 12 h light/dark cycle in the Institute Animal Facility room in Indian Association for the Cultivation of Science (IACS). The temperature of the room was maintained at ~24 °C and the humidity was maintained at ~50%. All the experiments were performed in accordance with the ethical guidelines as prescribed under IACS/IAEC/2018/04. Balb/c mice (8 weeks old, male) were subcutaneously injected with 100 µL of CT26 (mouse colon carcinoma) cell suspension on the right flank maintaining an inoculum of 3 million cells/mouse. Clear tumors were observed after 9/10 days of injection. When the tumors were reached at the volume of ~100 mm<sup>3</sup>, mice were divided into three groups (four mice per group). One group was kept as control and other two groups were given intra-tumoral injections of MXT-PER@PDA-COF-1 and HSA-MXT-PER@PDA-CON-1 respectively where final concentration of Mitoxantrone in stock formulation was maintained at 1.25 mg/mL and injected (4µL/gm body) weight on the 9<sup>th</sup> day from the carcinoma cell injection. During treatment, tumor volume was measured every 3 days by using a calliper and calculated as

$$\text{Tumor volume} = 4\pi/3 \times (\text{tumor length}/2) \times (\text{tumor width}/2)^2$$

After 24 days from the chemotherapeutic (MXT-PER@PDA-COF-1, HSA-MXT-PER@PDA-COF-1) injections, the mice were subjected for euthanasia and tumors were excised.

The tissues from various organs were collected, sliced and dehydrated successively and embedded in liquid paraffin and then were sliced into 3–5 mm for H&E staining Histological experiments were performed using the excised for tumors, kidneys, hearts, livers, lungs.

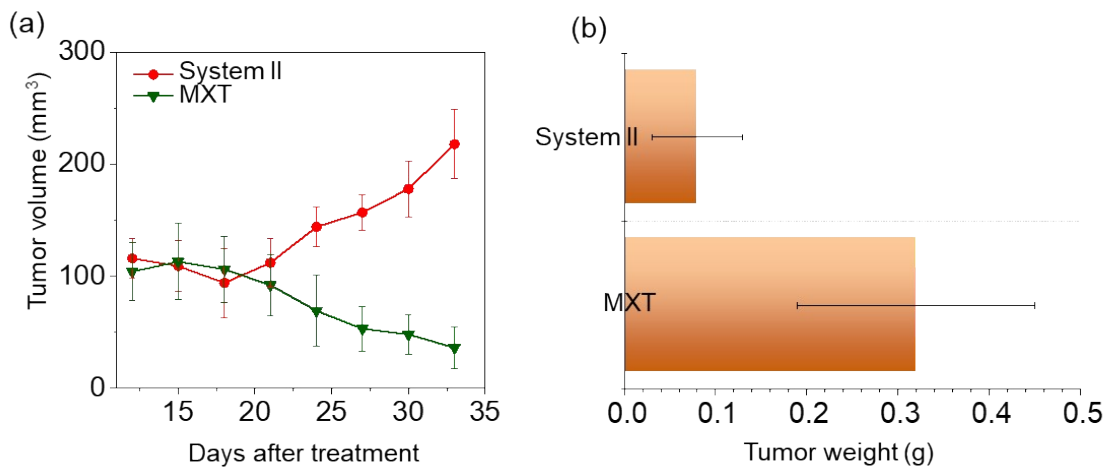


**Figure S25.** (a) Corresponding growth curves of tumors for MXT only (red) and System II (green plot); (b) Final tumor weights of the mice treated with MXT only and System II.

	7 days	15 days	30 days	Ideal range
<b>Haemoglobin</b>	12.1±1.6 g/dL	12.4±2.1 g/dL	11.8±1.9 g/dL	11-19.2 g/dL
<b>RBC</b>	7.9×10 <sup>6</sup> ±1.1/mL	8.1×10 <sup>6</sup> ±1.3/mL	7.6×10 <sup>6</sup> ±1.8/mL	6.36-9.42×10 <sup>6</sup> /mL
<b>WBC</b>	8.8×10 <sup>3</sup> ±0.7/mL	7.1×10 <sup>3</sup> ±0.8/mL	6.2×10 <sup>3</sup> ±0.4/mL	0.8-6.8×10 <sup>3</sup> /mL
<b>Platelet Count</b>	366×10 <sup>3</sup> ±34/mL	520×10 <sup>3</sup> ±25/mL	666×10 <sup>3</sup> ±42/mL	450-1590×10 <sup>3</sup> /mL
<b>RDW</b>	~15%	~16%	~16%	13-17%

#### Section S24: Blood biochemistry study:

Table S2. Haematology

Test	Test value	Ideal range
<b>Neutrophils</b>	~20%	10-30%
<b>Lymphocytes</b>	~76%	65-85%
<b>Monocytes</b>	~3%	0-5%
<b>Eosinophils</b>	~1%	0-6%
<b>Basophils</b>	0%	0-1%
<b>Mean Corpuscular Volume (MCV)</b>	47.6±3 fL	48.2-58.3 fL
<b>Mean Corpuscular Haemoglobin</b>	15.4±1.5 pg	15-19 pg

<b>Mean Corpuscular Haemoglobin Conc. (MCHC)</b>	32.4 ± 2.2 g/dL	30.2-35.3 g/dL
<b>Packed Cell Volume (PCV)</b>	36.4%	34.6-44.6%

Table S3. Differential count

	<b>System-I (7 day)</b>	<b>System-II (7 day)</b>	<b>System-I (15 day)</b>	<b>System-II (15 day)</b>	<b>System-I (30 day)</b>	<b>System-II (30 day)</b>	<b>Ideal Range</b>
<b>BUN</b>	44 mg/dL	30.8 mg/dL	41.5 mg/dL	27.8 mg/dL	37 mg/dL	24.4 mg/dL	Upto 45 mg/dL
<b>Creatinine</b>	0.7 mg/dL	0.28 mg/dL	0.51 mg/dL	0.22 mg/dL	0.42 mg/dL	0.17 mg/dL	0.097-0.184 mg/dL

Table S4. Kidney Index

	<b>System-I (7 day)</b>	<b>System-II (7 day)</b>	<b>System-I (15 day)</b>	<b>System-II (15 day)</b>	<b>System-I (30 day)</b>	<b>System-II (30 day)</b>	<b>Ideal Range</b>
<b>AST</b>	750 U/L	485 U/L	660 U/L	410 U/L	515 U/L	355 U/L	30-380 U/L
<b>ALT</b>	84 U/L	58 U/L	67 U/L	42 U/L	67 U/L	34 U/L	17.5-30.2 U/L

Table S5. Liver Index

### Section S25: Preparation of tissue lysate and bio-distribution studies

After treatments, mice were properly euthanized and its organs (spleen, kidneys, liver, lungs, and heart) and tumors (for tumor bearing mice) were extracted. Then, those were washed with 0.9% NaCl solution at 4 °C and conserved at -80 °C after immersion in liquid nitrogen. The organs were homogenized in PBS buffer (pH 7.4) and the resulting solution was collected for further spectroscopic studies. Same amount of each tissue was homogenized for preparing the lysates. Fluorescence of MXT ( $\lambda_{\text{max}} = 685 \text{ nm}$ ) was measured in each tissue lysate to check the distribution profile

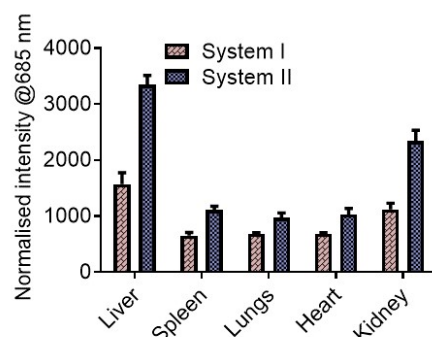


**Figure S26.** Distribution of MXT in major organs upon intravenous administration non-tumor bearing mice.

## Section S26 Clearance Pathway

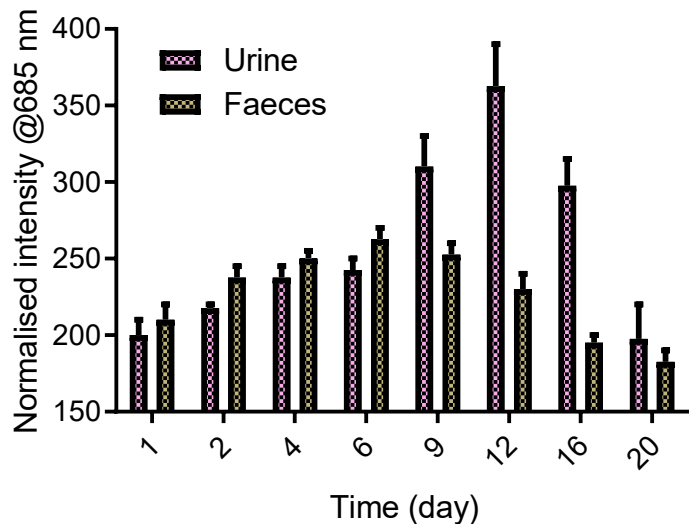


**Figure S27.** Detection of MXT in urine and faeces at various time intervals after injection of HSA-MXT-PER@PDA-COF-1

## References

- (1) M. A. Addicoat, D. E. Coupry and T. Heine, *J. Phys. Chem. A*, 2014, **118**, 9607-9614.
- (2) B. Aradi, B. Hourahine and T. Frauenheim, *J. Phys. Chem. A*, 2007, **111**, 5678-5684.
- (3) M. Elstner, D. Porezag, G. Jungnickel, J. Elsner, M. Haugk, T. Frauenheim, S. Suhai and G. Seifert, *Phys. Rev., B* 1998, **58**, 7260-7268.
- (4) M. A. Addicoat, S. Fukuoka, A. J. Page and S. Irle, *J. Comput. Chem.*, 2013, **34**, 2591-2600.